

Polyketide Synthase-Mediated O-Methyloxime Formation in the Biosynthesis of the Oximidine Anticancer Agents

Eveline Vriens^{+[a,b]}, Dries De Ruyscher^{+[a,b]}, Angus N.M. Weir^[a,b], Sofie Dekimpe^[a,b], Gert Steurs^[c], Ahmed Shemy^[d], Leentje Persoons^[e], Ana Rita Santos^[f], Christopher Williams^[g], Dirk Daelemans^[e], Matthew P. Crump^[g], Arnout Voet^[d], Wim De Borggraeve^[h], Eveline Lescrinier^[i] and Joleen Masschelein*^[a,b]

- [a] E. Vriens, Dr. D. De Ruyscher, Dr. A. Weir, Dr. S. Dekimpe, Prof. J. Masschelein
Laboratory for Biomolecular Discovery and Engineering, Department of Biology, KU Leuven, 3001 Heverlee, Belgium
E-mail: joleen.masschelein@kuleuven.be
- [b] E. Vriens, Dr. D. De Ruyscher, Dr. A. Weir, Dr. S. Dekimpe, Prof. J. Masschelein
VIB-KU Leuven Center for Microbiology, 3001 Heverlee, Belgium
- [c] Dr. G. Steurs
Department of Chemistry, KU Leuven, 3001 Heverlee, Belgium
- [d] A. Shemy, Prof. A. Voet
Laboratory for Biomolecular Modelling and Design, Department of Chemistry, KU Leuven, 3001 Heverlee, Belgium
- [e] L. Persoons, Prof. D. Daelemans
Laboratory of Virology and Chemotherapy, Rega Institute for Medical Research, KU Leuven, 3000 Leuven, Belgium
- [f] Dr. A. R. Santos
VIB Discovery Sciences, 3001 Heverlee, Belgium
- [g] Dr. C. Williams, Prof. M.P. Crump
School of Chemistry, University of Bristol, BS8 1TS Bristol, United Kingdom
- [h] Prof. W. De Borggraeve
Sustainable Chemistry for Metals and Molecules, Department of Chemistry, KU Leuven, 3001 Heverlee, Belgium
- [i] Prof. E. Lescrinier
Laboratory for Medicinal Chemistry, Rega Institute for Medical Research, KU Leuven, 3000 Leuven, Belgium
- [+] These authors contributed equally
- [*] Corresponding author

Abstract: Bacterial *trans*-acyltransferase polyketide synthases (*trans*-AT PKSs) are modular megaenzymes that employ unusual catalytic domains to assemble diverse bioactive natural products. One such PKS is responsible for the biosynthesis of the oximidine anticancer agents, oxime-substituted benzolactone enamides that inhibit vacuolar H⁺-ATPases. Here, we describe the identification of the oximidine gene cluster in *Pseudomonas baetica* and the characterization of four novel oximidine variants, including a structurally simpler intermediate that retains potent anticancer activity. Using a combination of *in vivo*, *in vitro* and computational approaches, we experimentally elucidate the oximidine biosynthetic pathway and reveal an unprecedented mechanism for O-methyloxime formation. We show that this process involves a specialized monooxygenase and methyltransferase domain and provide insight into their activity, mechanism and specificity. Our findings expand the catalytic capabilities of *trans*-AT PKSs and identify potential strategies for the production of novel oximidine analogues.

Introduction

Polyketides and nonribosomal peptides are two major classes of microbial specialized metabolites with highly diverse chemical structures and important applications in medicine and agriculture.^[1,2] They are constructed through stepwise condensation of simple monomeric building blocks by large enzymatic assembly lines, known as polyketide synthases (PKSs) and nonribosomal peptide synthetases (NRPSs).^[3] Most PKSs and NRPSs have a modular architecture, each module consisting of a set of catalytic domains responsible for the incorporation of one building block and a varying range of modifications into the growing chain. In PKSs, acyltransferase

(AT) domains select and load short carboxylic acid precursors onto the phosphopantetheinyl prosthetic arm of acyl carrier protein (ACP) domains, while ketosynthase (KS) domains catalyze the condensation reactions between the ACP-bound substrates and the growing polyketide chain.^[4] NRPSs, on the other hand, employ adenylation (A) domains to activate and load a diverse range of (non-)proteinogenic amino acids onto peptidyl carrier protein (PCP) domains, and condensation (C) domains to catalyze chain elongation.^[3] In both types of assembly lines, a variety of additional domains may be present that further modify the growing peptide or polyketide chain. During this assembly process, all biosynthetic intermediates remain covalently tethered to the ACP and PCP domains as thioesters. The final PKS or NRPS module often harbors a thioesterase (TE) domain at its C-terminus that releases the fully assembled chain via macrocyclization or hydrolysis.^[5]

A rapidly expanding and phylogenetically distinct group of PKSs, called *trans*-AT PKSs, does not adhere to this textbook biosynthetic model.^[6] *Trans*-AT PKSs lack integrated AT domains in their modules and instead use a single, *trans*-acting AT domain for substrate selection and loading. They are also known to exhibit remarkable architectural diversity, with pathways containing split or non-elongating modules, diverse *trans*-acting enzymes, novel domains performing unusual catalytic chemistry and non-canonical domain orders.^[6] Due to these atypical features, *trans*-AT PKSs do not only carry significant potential for the discovery of novel drug leads, but also represent a rich source of novel chemistry and enzymology.

The oximidines are hybrid polyketide-nonribosomal peptide antitumor agents produced by *Pseudomonas* spp. (**Figure 1A**).^[7-9] They belong to the benzolactone enamide family of

vacuolar H⁺-ATPase (V-ATPase) inhibitors.^[10] V-ATPases are ATP-driven proton pumps that control pH homeostasis in eukaryotic intracellular compartments to enable essential cellular processes, such as protein degradation and membrane trafficking. Their malfunctioning is associated with a range of human diseases, including cancer, osteoporosis and neurodegeneration.^[11] The oximidines selectively inhibit mammalian-type V-ATPases and show potent anticancer activity at nanomolar concentrations.^[7,9,10,12,13]

All benzolactone enamides share a common scaffold, composed of a salicylic acid residue and an enamide side chain that are connected by a macrolactone ring of variable length and composition (**Figure 1B and 1C**). Despite their promising biological activity, the genetic basis for the biosynthesis of benzolactone enamides in bacteria has remained elusive for many years. Only recently, during the preparation of our manuscript, the necroxime and lobatamide gene clusters were identified in the genome of *Burkholderia* and *Gyvuella* bacteria, respectively, and a plausible pathway for their biosynthesis was proposed.^[14,15] Moreover, using a targeted genome mining approach, related pathways were discovered in diverse bacterial phyla, including a putative oximidine biosynthetic gene cluster in *Pseudomonas* and *Chromobacterium* bacteria.^[14] Benzolactone enamides are constructed by multimodular *trans*-AT PKS-NRPS assembly lines that have several unusual features, including non-canonical domains and atypical chain termination modules. Several of these pathways, including the one that assembles the oximidines, also incorporate an O-methyloxime moiety (**Figure 1**), a functional group that is rarely found in specialized metabolites and is almost exclusively installed by post-assembly tailoring enzymes.^[16–18] Oxime formation in benzolactone enamides likely proceeds through an unprecedented mechanism, involving oxidation of the glycine starter unit by a unique oxygenase-containing module at the beginning of the assembly line.

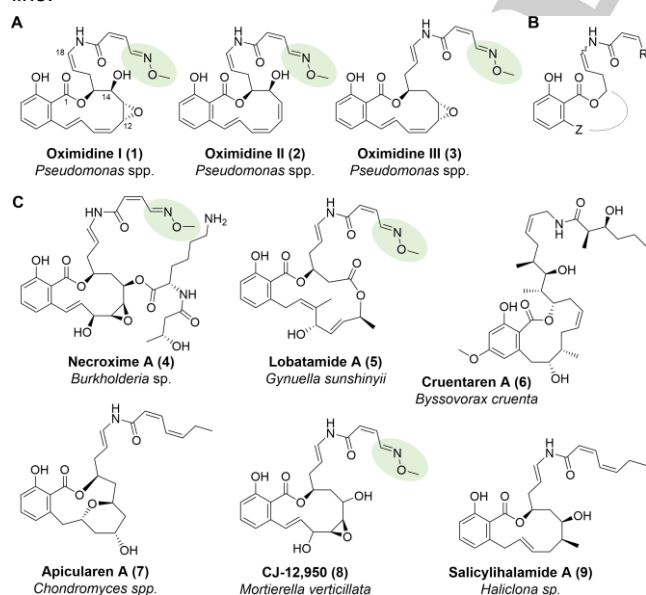


Figure 1. Structures of known benzolactone enamides. A) Structures of oximidine I–III (1–3), previously identified as metabolites of *Pseudomonas* spp. B) Common scaffold shared by all benzolactone enamides. C) Structures of other benzolactone enamides, isolated from diverse organisms. The O-methyloxime moiety in the oximidines, lobatamides, necroximes and CJ-12,950 is highlighted in green.

Here, we report a combination of bioinformatics analyses, targeted gene deletions, enzyme activity assays, docking studies and molecular dynamics simulations that illuminate the oximidine biosynthetic pathway, including its unique mechanism of oxime formation. We discover three novel oximidine variants and experimentally elucidate the functional role of each gene involved in oximidine biosynthesis. By manipulating the biosynthetic pathway, we also identify a structurally simplified oximidine intermediate that retains potent anti-cancer activity. Finally, we elucidate the catalytic activity, mechanism and specificity of the enzymes involved in O-methyloxime formation, further expanding the catalytic repertoire of PKS domains in *trans*-AT PKSs.

Results and Discussion

Identification and Structure Elucidation of the

Oximidines

During an *in silico* screen of *Pseudomonas* spp. for biosynthetic novelty, *P. baetica* a390T, originally isolated from the liver of a diseased fish,^[19] was found to contain a ± 60 kb cryptic biosynthetic gene cluster (BGC) encoding a hybrid *trans*-AT PKS/NRPS assembly line with unusual domains and non-canonical domain architectures (**Figure 2A**). The cluster comprises ten core biosynthetic genes (*oxiA–J*), which are flanked by several genes encoding putative tailoring enzymes and regulation-related proteins (**Table S1**). To identify the metabolic product of this cryptic gene cluster, we inactivated the *oxiB* gene by insertional mutagenesis. UHPLC-ESI-Q-TOF-MS analysis of ethyl acetate extracts from cultures of *P. baetica*, grown for three days in minimal medium, identified five metabolites whose production was abolished in the Δ *oxiB* mutant: two metabolites with the molecular formula C₂₃H₂₄N₂O₇ (calculated for C₂₃H₂₅N₂O₇⁺: 441.1661, found: 441.1655 and 441.1653), two with the molecular formula C₂₃H₂₄N₂O₆ (calculated for C₂₃H₂₅N₂O₆⁺: 425.1712, found: 425.1706 and 425.1718) and one with the molecular formula C₂₃H₂₄N₂O₅ (calculated for C₂₃H₂₅N₂O₅⁺: 409.1763, found: 409.1757) (**Figure S1**). The first molecular formula is consistent with oximidine I (1), and the second with oximidine II (2) and III (3), previously reported as metabolites of *Pseudomonas* sp. Q52002 and QN05727.^[7,8] To identify the metabolites from *P. baetica* a390T, large-scale cultures of the strain were grown in minimal medium and ethyl acetate extracts of the supernatant were fractionated by preparative HPLC (**Figure S2**).

The planar structure of the purified metabolites was elucidated using a combination of ¹H, ¹³C, COSY, TOCSY, HSQC, HMBC, NOESY and ROESY experiments (**Figure S3–S22, Table S2–S5**). These data revealed that *P. baetica* a390T indeed produces oximidine I (1), along with three novel oximidine congeners (**11–13, Figure 2**) that have not previously been isolated from a natural source. The fifth metabolite with molecular formula C₂₃H₂₄N₂O₅ could not be purified in sufficient quantity and purity for NMR spectroscopic analysis. The structure of **11** was found to be identical to oximidine III, except for the configuration of the enamide double bond. ³J_{HH} coupling constants of 7.2 Hz for H-

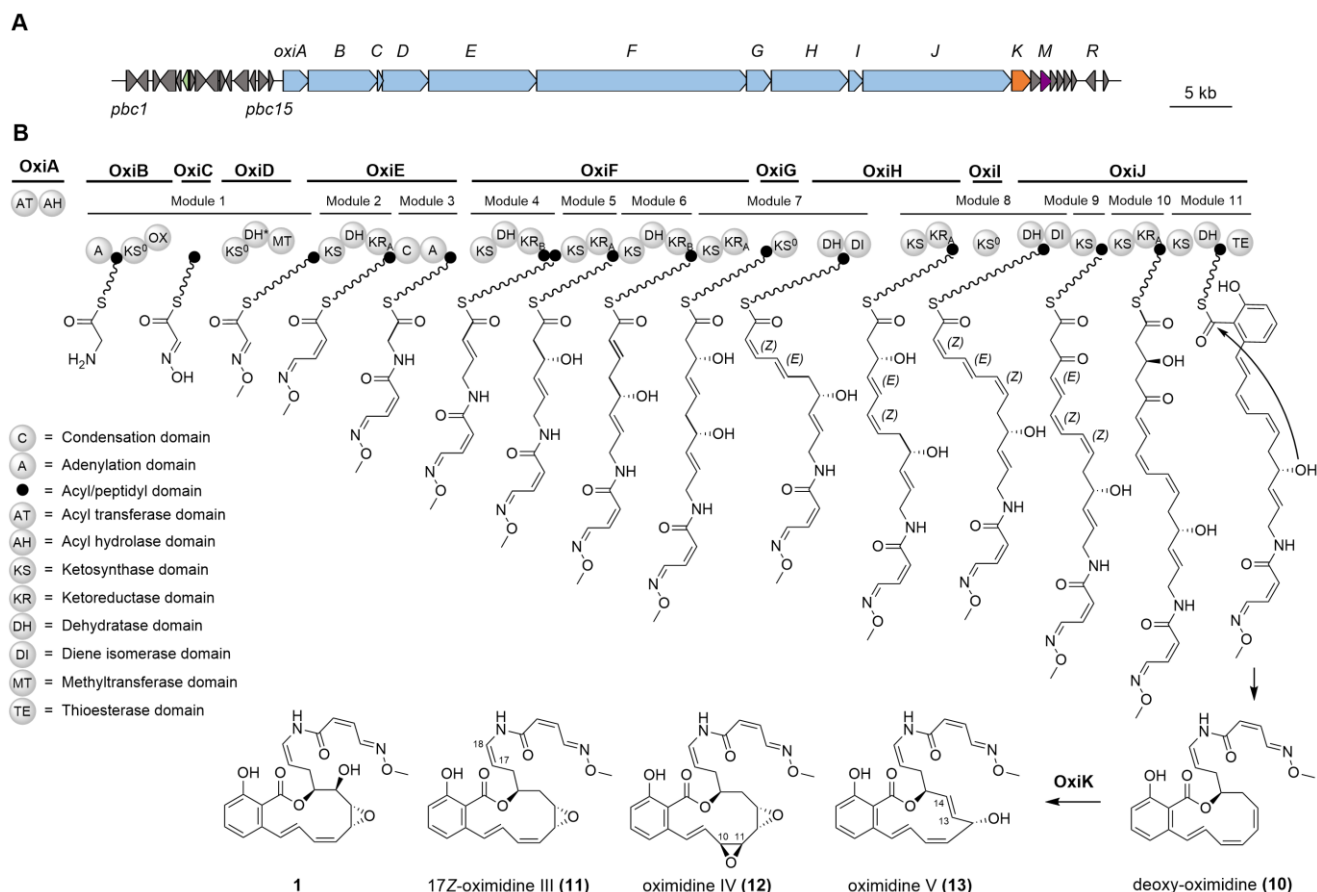


Figure 2. Organization of the oximidine biosynthetic gene cluster (*oxiA-M*) and proposed pathway for oximidine biosynthesis. A) Genetic organization of the gene cluster that directs the biosynthesis of the oximidines in *P. baetica* a390T. The genes encoding the modular trans-AT PKS/NRPS, the cytochrome P450 and the phosphopantetheinyl transferase are highlighted in blue, orange and purple, respectively. B) The proposed roles played by the OxiA-J modular PKS and the OxiK cytochrome P450 in oximidine biosynthesis. The proposed structures of the ACP-bound thioester intermediates following α - and β -carbon processing are presented. The predicted stereospecificity of KR domains is denoted as type A or B in subscript. The precise timing of the C17-C18 double bond shift remains to be elucidated.

17/H-18 indicated that the C-17/C-18 double bond has the Z-configuration. The structure of **11** was further confirmed by comparison with spectroscopic data previously reported for the chemically synthesized Z-enamide stereoisomer of oximidine III (**3**).^[20] For the other two newly identified oximidines, which we named oximidine IV (**12**) and V (**13**), three networks of COSY correlations were observed, which established the structures of the C-4 to C-6, C-8 to C-18 and C-20 to C-22 fragments. HMBC correlations between C-19 and the protons of C-18, C-20 and C-21, between the C-8 proton and C-6 and C-7, and between H-9 and C-7, allowed the position of the amide carbonyl and the connectivity between the phenol and the macrolactone ring to be determined (Figure S10,S16). HMBC correlations further confirmed the location of the C-1 ester, C-3 hydroxyl and the oxime methyl group. Based on $^3J_{\text{HH}}$ coupling constants of 8.1-8.4 and 10.8-10.9 Hz, the C-17/C-18 and C-20/C-21 double bonds were assigned the Z configuration, whereas coupling constants of 16.5-16.2 Hz are consistent with an E configuration for the C-8/C-9 double bonds. Signals at 52.35, 54.72, 56.29 and 56.51 ppm in the ^{13}C NMR spectrum and $^3J_{\text{HH}}$ coupling constants of around 3.5 Hz for H10-H13 showed that **12** contains two epoxide groups (Table S4). NOESY correlations between H-10 and H-11, and $^3J_{\text{HH}}$ coupling constants of > 3.4 Hz for H-10/H-11

and H-12/H-13 are indicative of a cis-configuration in both epoxides. For **13**, extensive overlap in some multiplets was resolved by 1D TOCSY experiments starting with excitation of the multiplets corresponding to H16_{a/b} and the overlapping multiplet of H8/H21 at around 6.30 ppm (Figure S20). A $^3J_{\text{HH}}$ coupling constant of 15.6 Hz for H-13/H-14 and a signal at 72.06 ppm in the ^{13}C NMR spectrum led us to propose that **13** has a trans-configured double bond between C-13 and C-14, and a hydroxyl group at C-12, respectively (Table S5).

To assess the absolute stereochemistry of **12** and **13**, density functional theory (DFT) calculations were performed using the DP4+ approach proposed by Sarotti and co-workers.^[21] First, **12** and **13** were assumed to have the S-configuration at C-15, like all other previously reported oximidines and benzolactone enamides. In this scenario, four possible diastereomers of **12** were considered, with all epoxides in the cis-configuration. For **13**, two diastereomers were considered with either a (12R,15S) or a (12S,15S) configuration. Statistical comparison of the experimentally obtained ^1H and ^{13}C chemical shifts and the calculated values for all possible structures, enabled us to assign the (10S,11S,12S,13S)-diastereomer of **12** as the most

probable one, while **13** is proposed to correspond to the (12*R*,15*S*)-diastereomer.

The structure of oximidine V is quite unusual, with a *trans*-configured double bond between C-13 and C-14 that has not been observed in other benzolactone enamides. We thus sought to gain a better understanding of oximidine biosynthesis, including the diverse range of oxidation reactions and the mechanism for *O*-methyloxime formation.

Oximidine Biosynthesis

The OxiA-J hybrid PKS/NRPS shows a high degree of similarity to the lobatamide and necroxime assembly lines, as highlighted recently by Niehs *et al.* (Figure S21).^[14] Detailed analysis of the catalytic domains within the PKS and NRPS subunits allowed us to propose a plausible pathway for oximidine biosynthesis (Figure 2B). Like all *trans*-AT PKSs, OxiB-OxiJ lack integrated AT domains in their modules. A didomain AT-AT protein, OxiA, is encoded directly upstream of the PKS/NRPS genes. Phylogenetic analysis of these enzymes identified the N-terminal AT domain as an AT with specificity for malonyl-CoA. In contrast, the C-terminal AT-like domain clades with acyl hydrolase enzymes which are known to perform a proofreading function by removing stalled intermediates from ACP domains (Figure S22).^[22] Sequence analysis of the A domains in OxiB and OxiE using antiSMASH confirmed that they both activate *L*-glycine.^[23] The configuration of the hydroxyl-bearing stereocenters was predicted from sequence analysis of the KR domains within OxiE, OxiF, OxiH and OxiJ (Table S6). Based on the structures of the oximidines, the OxiB, OxiD, OxiG and OxiI KS domains are all hypothesized to transfer acyl intermediates from one ACP or PCP domain to the next, without elongating them. This hypothesis is supported by phylogenetic analyses, which place these KS domains in clades along with other non-elongating KS⁰ domains (Figure S23A). The OxiD, OxiG and OxiI KS domains also lack the conserved His residue required for decarboxylative condensation (Figure S23B).

The early stages in oximidine biosynthesis appear to mirror those in the formation of the necroximes and lobatamides. The first module is proposed to be involved in the formation of the unusual *O*-methyloxime moiety. The amino group of the glycine starter unit is presumably oxidized by a specialized flavin-dependent monooxygenase (OX) domain within OxiB, and subsequently *O*-methylated by the OxiD methyltransferase domain (MT). Starting from module 2, the domain architecture of the oximidine assembly line starts to diverge from that of other benzolactone enamides. A striking feature that is unique to the oximidine and necroxime pathways is the presence of two type C dehydrating bimodules with the unusual domain sequence KS-KR_A-ACP-KS⁰-DH-ACP-DH (Figure S21). The C-terminal DH domain is hypothesized to function as a diene isomerase (DI) by interconverting α/β -*cis*, γ/δ -*trans* dienes with α/β -*trans*, γ/δ -*cis* dienes.^[24] The downstream KS domain may then perform a gatekeeping function by selecting the isomerized intermediate. Similar type C dehydrating bimodules have so far only been identified in the bongkrekic acid, sorangicin and diffidin pathways. Interestingly, the double bond predicted to be incorporated in module 4 is shifted in the final oximidine structures to form the enamide. It remains to be investigated

whether one of the DI domains is also involved in this double bond isomerization.

Release of the fully assembled polyketide-peptide chain is proposed to involve the formation of a salicylate moiety by the C-terminal DH domain within OxiJ, followed by TE domain-catalyzed macrolactonisation.^[14,15] This mechanism of chain release is common to all pathways within the benzolactone enamide family. An identical domain sequence appears to be responsible for generating a salicylate group in the biosynthesis of SIA7248 in *Streptomyces* sp. A7248.^[25] However, the resulting thioester intermediate is released from the assembly line by dimerization rather than cyclisation to form a homodimeric macrodiolide (Figure S24). The underlying factors that determine the differential outcome of the chain release reaction in these two types of pathways remain to be elucidated.

Following chain release, the benzolactone intermediates undergo a variable range of oxygenations, including epoxidation and hydroxylation, to yield the final, bioactive cytotoxins. These oxidative tailoring reactions are likely catalysed by the putative cytochrome P450 OxiK. To experimentally validate the role of OxiK, we created an in-frame deletion in the corresponding gene. The resulting mutant was unable to assemble oximidines **1**, **11**, **12** and **13**, but instead produced increased levels of the previously observed metabolite with molecular formula C₂₃H₂₄N₂O₅ (Figure 3, Figure S25). Complementation of this mutant via *in trans* expression of *oxiK* restored the production of all oximidines. The increased production of the unknown oximidine-related metabolite in the Δ *oxiK* mutant enabled us to purify it and elucidate its structure. NMR spectroscopic analysis showed that this metabolite is deoxy-oximidine (**10**), which lacks all hydroxyl and/or epoxide groups on the macrolactone ring (Figure 2, Figure S26-31, Table S7). This is consistent with the proposed role of OxiK as cytochrome P450 and post-assembly tailoring enzyme. The absence of a C13-14 *trans*-configured deoxy-oximidine congener in the Δ *oxiK* mutant indicates that the unusual configuration of oximidine V (**13**) is linked to the activity of OxiK. Cytochrome P450 enzymes are known to catalyze different oxidation and reduction reactions, including epoxidation, hydroxylation, C-C bond formation and cleavage, and desaturation.^[26] In the case of oximidine V, OxiK may first install a hydroxyl group at C-12. Subsequent hydrogen abstraction at C-13 or C-14 to generate a carbon radical could then be followed by rotation around the C-13/C-14 bond due to the low energy barrier between the two conformations. Finally, a second hydrogen abstraction would yield the *trans*-configured double bond.

We also examined whether the genes in direct proximity of *oxiA-K* play a role in oximidine biosynthesis, export or regulation. OxiM shows sequence similarity to 4'-phosphopantetheinyl transferases and is likely responsible for post-translational modification of the ACP and PCP domains within the assembly line via attachment of a coenzyme A (CoA)-derived phosphopantetheinyl (Ppant) prosthetic group. To test this hypothesis, we constructed an in-frame deletion in *oxiM*. LC-MS comparison of extracts from the wild type and mutant strain confirmed that oximidine production is abolished in the mutant (Figure S32). Complementation of this deletion by *in trans* expression of *oxiM* restored oximidine biosynthesis.

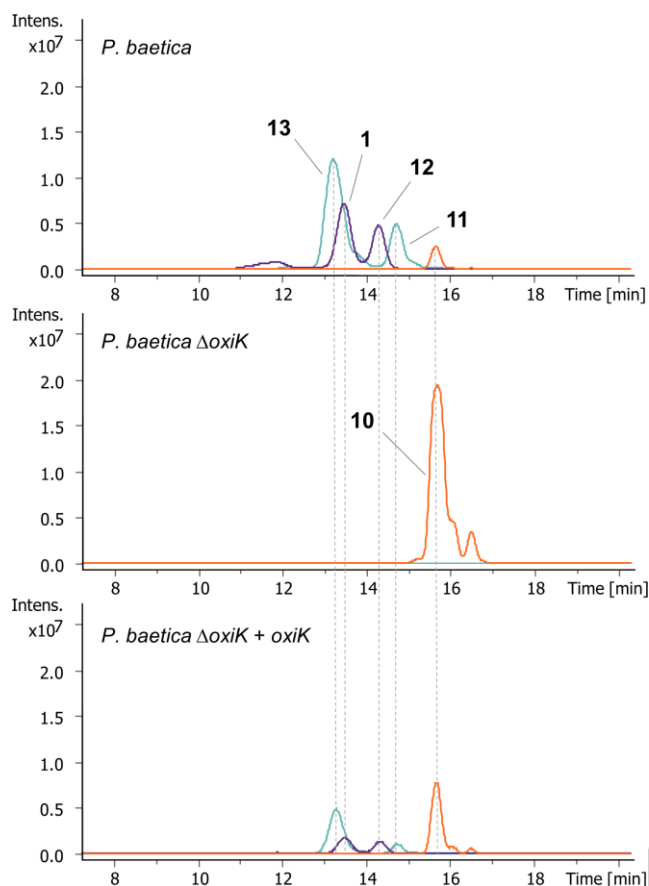


Figure 3. The effect of *oxiK* deletion on oximidine production in *P. baetica* a390T. Extracted ion chromatograms at $m/z = 425.1706$ (turquoise, corresponding to the $[M+H]^+$ ion for oximidine III and oximidine V), $m/z = 442.1655$ (purple, corresponding to the $[M+H]^+$ ion for oximidine I and oximidine IV) and $m/z = 409.1763$ (orange, corresponding to the $[M+H]^+$ ion for deoxy-oximidine) from UHPLC-ESI-Q-TOF-MS analyses of culture extracts from wildtype *P. baetica* a390T (top), the $\Delta oxik$ mutant (middle) and the $\Delta oxik$ mutant complemented by *in trans* expression of *oxiK* (bottom).

Other genes located directly up- and downstream of *oxiA-J* encode proteins that show sequence similarity to metallophosphoesterases (OxiL), choline dehydrogenases (OxiQ), transcriptional regulators (OxiP and Pbc5), helicases (Pbc9), serine/threonine-protein kinases (Pbc4) and methyltransferases (Pbc1 and Pbc2). Thirteen genes (*oxiNOP*, *pbc3*, *pbc6-8* and *pbc10-15*) did not possess any significant similarity to sequences in the public databases and were listed as hypothetical proteins (Figure 2, Table S1). To probe their role in oximidine biosynthesis, we constructed individual, in-frame deletions in each of these genes. LC-MS analysis showed that oximidine production was unaffected in all mutants, indicating that these genes probably do not form part of the oximidine gene cluster.

The OxiB OX and the OxiD MT Domain Are Involved In

O-methylxime Formation

To the best of our knowledge, O-methylxime formation by embedded flavin-dependent monooxygenase and

methyltransferase domains is unprecedented in PKS enzymology. We thus sought to experimentally validate the proposed role of these enzymes by using a combination of *in vitro*, *in vivo* and *in silico* approaches.

The O-methylxime assembly process is proposed to be initiated by loading of glycine onto the Ppant prosthetic arm of the PCP domain within OxiB (Figure 2 and 4A). The adjacent KS^0 domain is then hypothesized to shuttle the glycine thioester to the OxiC ACP domain where the OX domain of OxiB oxidizes the glycine amino group to the corresponding oxime via a hydroxylamine and nitroso intermediate. Sequence alignments and phylogenetic analysis revealed that the OX domain belongs to the class B flavoprotein monooxygenases (FMOs) which contain two Rossmann folds, one for the binding of FAD and one for NADPH, as well as a characteristic FMO sequence motif (FxGxxxHxxxY) (Figure S33A).^[29,30] Within the class B FMOs, the OxiB OX domain groups together with the corresponding domains from the necroxime and lobatamide pathways in a separate clade within the type I FMO subclass (Figure S34). Following oxime formation, a second KS^0 domain appended to the N-terminus of OxiD likely transfers the intermediate to the ACP domain within OxiE. Next, a putative S-adenosyl methionine (SAM)-dependent methyltransferase domain at the C-terminus of OxiD is believed to be responsible for methylation of the oxime group. This hypothesis is supported by phylogenetic analysis which shows that the OxiD MT domain clusters with other O-methyltransferases (Figure S35). Notably, a DH-like (DH*) domain containing a double hotdog fold is positioned directly upstream from the MT domain in the oximidine and necroxime pathways. However, the lobatamide assembly line lacks this domain (Figure S21). This observation, together with the absence of key catalytic residues (Figure S33B) and the fact that it clades with catalytically inactive DH domains (Figure S36) suggests that this DH* domain may not be involved in O-methylxime formation.

To establish whether the OX, MT and DH* domain within OxiB and OxiD are required for oxime formation, we individually inactivated each domain in *P. baetica* via site-directed mutagenesis. To inactivate the OX domain, we replaced the second glycine (G1213) in the FAD binding motif (GXGXG) with a bulky, negatively-charged aspartic acid residue to repel the negatively charged phosphate groups of FAD. The activity of the MT domain was abolished by mutating a conserved acidic residue (D976V) that forms hydrogen bonds to both hydroxyl groups in the ribose ring of SAM.^[31] The OxiD DH* domain lacks the His-Asp catalytic dyad typically found in DH domains. However, other DH-like domains, such as enoyl isomerases, have been shown to use a single catalytic His residue that is positioned differently from that of conventional DH domains.^[32] We therefore performed a multiple sequence alignment with similar DH* domains found in the necroxime and other putative oximidine pathways and identified one conserved His residue, which we mutated to alanine (H710A) (Figure S33C). UHPLC-ESI-Q-TOF-MS analyses of extracts from culture supernatants showed that oximidine production is abolished in the *oxiB* OX and *oxiD* MT mutants. In contrast, no effect on oximidine production was observed in the *oxiD* DH* mutant. These results indicate that only the OX and MT domain play an essential role in O-methylxime formation during oximidine assembly (Figure

S37). Upon feeding of (^{13}C -Me)-*L*-methionine to small-scale cultures of *P. baetica* a390T, a mass increase of 1 Da was observed for all oximidines, providing further confirmation that SAM is the source of the oxime methyl group (**Figure S38**).

The OxiB OX Domain Catalyzes Oxime Formation

To investigate the function of the OxiB OX domain, we overproduced the ACP domains of OxiB, OxiC and OxiE, and the OxiB OX domain in *E. coli* as N- or C-terminal His₆ fusion proteins and purified them to homogeneity (**Figure S39 and S40**). UHPLC-ESI-Q-TOF-MS analysis confirmed that all purified proteins had the expected molecular weight (**Figure S39**). The UV-Vis spectrum of the purified OX domain showed two absorbance maximums at 375 and 450 nm, which is consistent with the presence of FAD (**Figure S41**). To convert the OxiB, OxiC and OxiE ACP domains into their *holo*-form, the proteins were incubated with CoA and purified recombinant Sfp, a promiscuous phosphopantetheinyl transferase from *Bacillus subtilis* (**Figure S42**).^[33] To investigate the catalytic activity of the OX domain, we synthesized the *N*-acetylcysteamine (SNAC) thioester of *L*-glycine as a simplified mimic of the ACP-bound starter unit. The glycine substrate was then transferred onto the Ppant arm of the *holo*-OxiC ACP domain through transthioesterification (**Figure S43**). After removing the excess glycyl-SNAC, the acylated ACP domain was incubated with the OxiB OX domain, FAD and NADPH to examine whether the OX domain can oxidize the glycine amino group. UHPLC-ESI-Q-TOF-MS analysis of the resulting mixture showed that the ACP-bound glycine had undergone oxidation to the corresponding oxime (**Figure 4B**). The identity of the reaction product was confirmed via the Ppant ejection assay, which yielded an ion at m/z 332.1287, corresponding to a Ppant-bound oxime species.^[34] In contrast, no oxime formation was detected when the OX domain was omitted from the reaction (**Figure 4B**), or when the *holo*-OxiC ACP domain was substituted with the *holo*-OxiB or -OxiE ACP domain (**Figure S44**). These data are consistent with the hypothesis that the OX domain catalyzes oxime formation when the glycine substrate is tethered to the OxiC ACP domain.

To unambiguously confirm the structure of the oxime product, we synthesized the SNAC derivative of ^{15}N -labelled *L*-glycine. Both the labelled and unlabelled glycyl-SNAC thioesters were then combined in separate, large-scale reactions with the OxiB OX domain, FAD, NADPH and, after 1.5 hours of incubation, 5% D₂O. ^1H , [^1H , ^{13}C]-HSQC and [^1H , ^{15}N]-HMBC NMR spectroscopic analyses of the resulting reaction mixtures showed that the signals attributed to the C $_{\alpha}$ protons of glycine disappeared in the ^1H NMR spectrum of the reaction with the unlabelled substrate (**Figure S45A**). Instead, two singlets at 7.10 and 7.11 ppm appeared, each integrating for one proton. HSQC correlations were observed between these protons and two ^{13}C signals at 146.5 and 146.7 ppm which can be assigned to the alpha carbons of an *E*- and *Z*-configured oxime product (**Figure S45B**).^[35,36] The C $_{\alpha}$ proton signals were split further into doublets in the ^1H NMR spectrum of the reaction with the labelled substrate, due to coupling to ^{15}N ($^3J_{15\text{N}-1\text{H}} = 2.5$ Hz). This was confirmed by the observation of a clear HMBC correlation between the C $_{\alpha}$ protons of the oxime products and the ^{15}N atoms (**Figure S45B**). It remains to be investigated whether the

OX domain is also capable of synthesizing the *Z* isomer of the oxime when the glycine substrate is attached the ACP domain, and whether one of the downstream KS domains acts as a gatekeeper by selecting only the *E*-configured oxime. In a complementary approach, we also synthesized the unstable *E*-configured oxime derivative of *L*-glycyl-SNAC. UHPLC-ESI-Q-TOF-MS analysis showed that this authentic standard has the same retention time as the product of the reaction of *L*-glycyl-SNAC with the OxiB OX domain, FAD and NADPH (**Figure S46**). No products with an m/z corresponding to the SNAC-linked oxime product could be detected in control reactions from which the OX domain was omitted. Together, these comparative structural analyses unambiguously confirm the identity of the oxime product.

Interestingly, UHPLC-ESI-Q-TOF-MS analysis of the reaction of *L*-glycyl-SNAC with the OX domain also identified a metabolite with a molecular formula corresponding to a hydroxylamine intermediate (calculated for C₆H₁₃N₂O₃S⁺: 193.0646, observed: 193.0641) (**Figure 4A, Figure S47**). The identity of this metabolite was investigated by derivatizing the reaction products with di-*tert*-butyl dicarbonate (BOC anhydride).^[37] LC-MS comparisons showed that the putative *N*-hydroxy-*L*-glycyl thioester intermediate had undergone conversion to a product with a molecular formula corresponding to a BOC-protected metabolite. These results provide further support for the presence of a hydroxylamine moiety in the proposed intermediate.

The OxiD MT Domain is Responsible for O-methylation of the Oxime Group

We next turned our attention to the MT domain of OxiD. To investigate its catalytic activity, the protein was overproduced in *E. coli* as an N-terminal His₆ fusion protein and purified to homogeneity. UHPLC-ESI-Q-TOF-MS analysis confirmed its identity (**Figure S39**). The ability of the MT domain to catalyze O-methylation was examined by loading the oxime substrate onto the Ppant prosthetic arm of the OxiE ACP domain. This was done by incubating the *holo*-ACP domain with the chemically-synthesized oxime derivative of *L*-glycyl-SNAC (**Figure 4C**). Although this transthioesterification reaction was successful, it was not very efficient due to the inherent instability of the oxime. After removing the excess SNAC thioester, the ACP-bound oxime substrate was incubated with the OxiD MT domain and SAM. UHPLC-ESI-Q-TOF MS analysis of the reaction mixture showed a mass shift consistent with the formation of an O-methylated product (**Figure 4C**). The identity of this product was confirmed via the Ppant ejection assay, which yielded an ion at m/z 346.1474, corresponding to a Ppant-bound O-methylloxime derivative of glycine. No methylation was observed when the MT domain was omitted from the reaction (**Figure 4C**), or when the *holo*-OxiE ACP domain was substituted with the *holo*-OxiC ACP domain (**Figure S48**). These results are consistent with the hypothesis that the MT domain catalyzes O-methylation of the oxime moiety after the oxime substrate is transferred to the OxiE ACP domain.

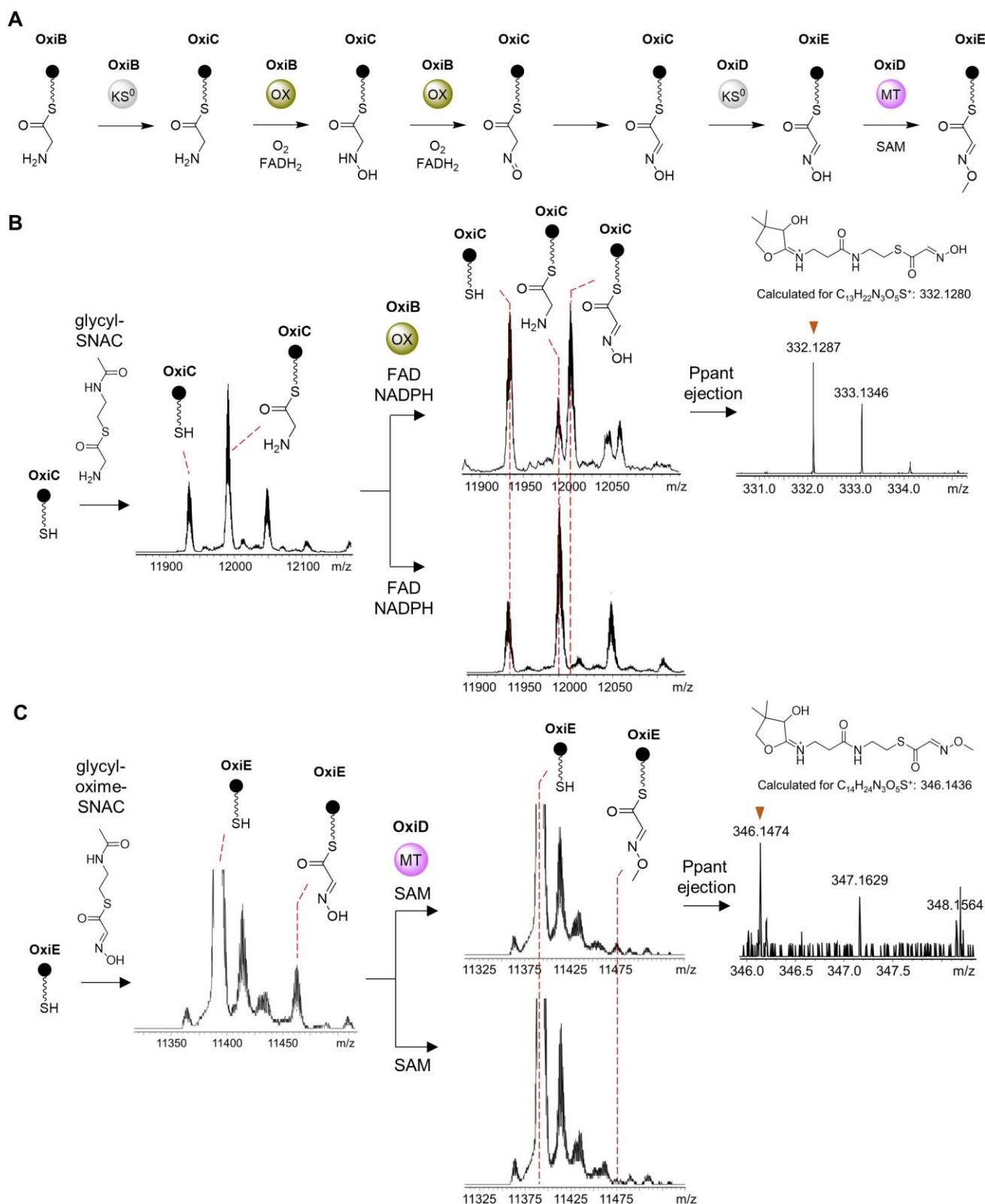


Figure 4. *In vitro* reconstitution of oxime formation and O-methylation by the OxiB OX and the OxiD MT domain, respectively. A) Proposed mechanism of O-methyloxime formation during oximidine biosynthesis. B) Deconvoluted mass spectra from incubation of the *holo*-OxiC ACP domain with *L*-glycyl-SNAC and subsequently, after washing away the excess SNAC-bound substrate, with the OxiB OX domain, FAD and NADPH. Control reactions were performed in the absence of the OX domain. The data demonstrate that the OX domain is able to oxidize the glycine substrate to the corresponding oxime. C) Deconvoluted mass spectra from incubation of the *holo*-OxiE ACP domain with the oxime derivative of *L*-glycyl-SNAC and, in a next step, with the OxiD MT domain and SAM. Methylation of the ACP-bound oxime is observed in the reaction mixture, but not in a control reaction from which the MT domain was omitted. The identity of the oxime and O-methyloxime products was confirmed using the Ppant ejection assay. The data shown are from a single measurement and are representative of three independent experiments.

The OxiD KS⁰ Domain Functions as a Carrier Protein

Transacylase

Having established the carrier protein specificity of the OX and MT domains, we next investigated the ability of the OxiD KS⁰ domain to transfer the oxime intermediate from the OxiC to the OxiE ACP domain. The KS⁰ domain was overproduced in *E. coli* and purified as described for the OX, ACP and MT domains. Initially, we loaded the oxime substrate onto the *holo*-OxiC ACP domain by incubating the protein with the chemically synthesized oxime derivative of *L*-glycyl-SNAC. To probe the acylation of the active site Cys residue in the OxiD KS⁰ domain during chain transfer, the KS⁰ domain was incubated with a 10-fold molar excess of the loaded OxiC ACP domain. Unfortunately, attempts to detect acyl transfer were unsuccessful due to the low efficiency of the initial OxiC loading reaction. To circumvent this problem, we directly loaded the oxime substrate onto the KS⁰ active site Cys residue by transthioesterification as described above. UHPLC-ESI-Q-TOF MS analysis confirmed that approximately 26% of the KS⁰ domain underwent acylation (Figure S49). After removal of excess SNAC thioester, equimolar amounts of the *holo*-OxiE ACP domain were added to the mixture to examine whether the KS⁰ domain can transfer the oxime substrate to the ACP domain. Analysis of the protein mixture by UHPLC-ESI-Q-TOF-MS showed that $\pm 10\%$ of the OxiE ACP domain underwent acetylation. Together, these data are consistent with the hypothesis that the OxiD KS⁰ domain is a carrier protein transacylase. Given that the OxiD MT domain is unable to interact productively with the OxiC ACP domain, the oxime intermediate must be translocated by the KS⁰ domain to the OxiE ACP domain for *O*-methylation to occur. This aligns well with a recent study that has shown that KS⁰ domains catalyze acyl transfer reactions to overcome ACP domain incompatibility.^[38]

The OxiB OX Domain Tolerates Alternative Aminoacyl

Substrates

In the context of the oximidine assembly line, the OX domain is naturally presented with a glycyl thioester substrate due to the strict selectivity of the A domain within OxiB. However, the OX domain may also accept other amino acids as substrates in the oxygenation reaction. To test this hypothesis, we incubated the OX domain with FAD, NADPH and a number of chemically synthesized aminoacyl-SNAC thioester analogues (Figure S50). UHPLC-ESI-Q-TOF-MS analysis of the reaction mixtures showed that alanyl- and threonyl-SNAC were well tolerated by the OX domain. In contrast, no hydroxylamine or oxime formation was observed when the enzyme was incubated with α -methylalanyl-SNAC. In the case of threonyl-SNAC, only production of the hydroxylamine derivative was observed, which may be due to the more bulky side chain of the amino acid.

In order to rationalize the observed substrate specificity, we generated a homology model of the OxiB OX domain and

performed docking and molecular dynamics (MD) simulations with the natural and alternate substrates. To more closely mimic the natural ACP-bound aminoacyl thioester substrate, we chose to dock the amino acids as pantetheine (Pant) rather than SNAC thioesters. Computational docking revealed that *L*-glycyl-Pant, *L*-alanyl-Pant and *L*-threonyl-Pant could be accommodated in the active site cavity of the OX domain and had top scoring poses that positioned the terminal amine towards and in close proximity to FAD and NADPH (Figure S51A). The *L*-threonyl-pantetheine pose was found to be slightly different than that of *L*-glycyl- and *L*-alanyl-Pant, with the amino group located closer to FAD than NADPH. In contrast, the α -methylalanyl-Pant substrate could only be accommodated in the active site in a pose that completely flipped the molecule and positioned the terminal amine away from the cofactors, which is not compatible with catalysis. Inspection of the substrate binding site indicates that a steric clash between the methyl group of α -methylalanyl-Pant and the isoalloxazine ring of FAD could hinder its binding in the active site. To verify the stability of *L*-glycyl-Pant, *L*-alanyl-Pant and *L*-threonyl-Pant in the active site and account for any induced fit, we performed 20 ns MD simulations of the OX domain in complex with FAD, NADPH and the pantetheine-coupled substrates. The stability of the substrates in the active site was confirmed by following a proxy distance across the trajectory between FAD and the α -carbon of *L*-glycyl-Pant, *L*-alanyl-Pant and *L*-threonyl-Pant (Figure S51B). Overall, these data show that the OxiB OX domain can tolerate aminoacyl substrate analogues, indicating that it has the potential to be exploited for the production of novel oximidine variants.

Biological Activity of the Oximidines

Oximidines I-III are known to exhibit potent antitumor activity by targeting the V₀ subunit of mammalian V-ATPases. We therefore evaluated the activity of our newly identified oximidine variants against a panel of cancer cells lines (Table 1). Among the variants tested, oximidine I (**1**) was found to be most effective in inhibiting tumor cell proliferation (CC₅₀: 0.15-970 nM), followed by oximidine V (**13**) (CC₅₀: 7.2-3250 nM), 17Z-oximidine III (**11**) (CC₅₀: 17-5160 nM) and oximidine IV (**12**) (CC₅₀: 420-17300 nM). Low nanomolar activity was detected against pancreatic adenocarcinoma, colorectal carcinoma and glioblastoma cells, while lung carcinoma and chronic myeloid leukemia cells showed less sensitivity. A significant yet reduced level of cytotoxicity towards peripheral blood mononuclear cells was observed (CC₅₀: 1060-37200 nM), indicating that the oximidines exhibit some selectivity towards cancer cells over normal cells.

Interestingly, deoxy-oximidine (**10**) exhibited cytotoxicity in a range comparable to oximidine V (CC₅₀: 7-2630 nM) (Table 1). This aligns well with previous reports indicating that the antitumor activity of benzolactone enamides is mainly determined by the presence of the enamide side chain^[27,28], the salicylate phenol^[28], the ring size and the *ortho*-substitution of the salicylate ester.^[28] The fact that **10** retains potent antitumor activity and can be obtained in good yields (4 mg/L), makes it an interesting starting point for further diversification of the oximidine scaffold by semi-synthetic approaches.

Table 1. CC50 values (μM) for oximidine I, 17Z-oximidine III, deoxy-oximidine, oximidine IV and oximidine V against a panel of cancer cell lines.

| Cancer cell line | Oximidine I (1) | Deoxy-oximidine (9) | 17Z-oximidine III (10) | Oximidine IV (11) | Oximidine V (12) |
|---------------------------------------|-----------------------|---------------------|------------------------|-------------------|---------------------|
| Capan-1 (pancreatic adenocarcinoma) | 0.00015 \pm 0.00007 | 0.0070 \pm 0.0014 | 0.017 \pm 0.001 | 0.42 \pm 0.06 | 0.0072 \pm 0.0011 |
| HCT-116 (colorectal carcinoma) | 0.013 \pm 0.001 | 0.036 \pm 0.019 | 0.069 \pm 0.042 | 1.31 \pm 0.72 | 0.037 \pm 0.015 |
| LN229 (glioblastoma) | 0.010 \pm 0.005 | 0.045 \pm 0.033 | 0.10 \pm 0.06 | 1.81 \pm 0.68 | 0.040 \pm 0.025 |
| NCI-H460 (lung carcinoma) | 0.10 \pm 0.02 | 4.40 \pm 3.54 | 5.16 \pm 2.47 | 6.2 \pm 3.26 | 3.25 \pm 0.21 |
| DND-41 (acute lymphoblastic leukemia) | 0.067 \pm 0.030 | 2.63 \pm 0.83 | 3.99 \pm 0.44 | 5.65 \pm 0.21 | 1.83 \pm 0.52 |
| HL-60 (acute myeloid leukemia) | 0.010 \pm 0.001 | 0.078 \pm 0.037 | 0.081 \pm 0.007 | 2.01 \pm 0.07 | 0.023 \pm 0.004 |
| K562 (chronic myeloid leukemia) | 0.970 \pm 0.523 | 4.34 \pm 2.06 | 4.5 \pm 2.41 | 17.30 \pm 5.23 | 2.97 \pm 0.43 |
| Z138 (non-Hodgkin lymphoma) | 0.017 \pm 0.004 | 0.10 \pm 0.01 | 0.12 \pm 0.02 | 2.37 \pm 0.04 | 0.053 \pm 0.011 |
| HepG2 (liver carcinoma) | 0.0316 \pm 0.0152 | 0.529 \pm 0.0176 | 0.453 \pm 0.0691 | 1.48 \pm 0.289 | 0.519 \pm 0.107 |
| Normal cells | | | | | |
| Peripheral blood mononuclear cells | 7.65 \pm 2.90 | 21.65 \pm 0.49 | 37.20 \pm 3.96 | 22.15 \pm 2.62 | 1.06 \pm 0.01 |

Conclusion

In summary, we have experimentally elucidated the biosynthetic pathway of the oximidine anti-cancer agents, oxime-substituted members of the benzolactone enamide family of mammalian V-ATPase inhibitors. Oximidine biosynthesis is directed by a hybrid *trans*-AT PKS/NRPS assembly line that harbors multiple unusual domains and atypical domain architectures. Our data provide evidence for an unprecedented mechanism for O-methyloxime formation during oximidine assembly, involving oxidation, transacylation and subsequent O-methylation of the glycine starter unit by a specialized flavin-dependent OX, KS⁰ and MT domain embedded within the PKS, respectively. Using a combination of *in vitro* biochemical assays, targeted gene inactivations, bioinformatics analyses, docking studies and MD simulations, we obtained detailed insights in the catalytic activity, mechanism and specificity of these enzymatic domains. We also show that the OX domain can tolerate alternative amino acid substrates, indicating that it may be possible to produce novel oximidine analogues by feeding aminoacyl-SNAC thioesters to mutants of *P. baetica* in which the N-terminal A or PCP domain within OxiB is inactivated. Apart from oximidine I, we also isolated and elucidated the structure of three novel oximidine variants that show comparable anti-cancer activity in the nano- to micromolar range. Furthermore, deoxy-oximidine, an oximidine variant that lacks all hydroxyl and/or epoxide groups on the macrolactone ring, was identified and implicated as a direct precursor to oximidines 1, 11, 12 and 13. Despite its simplified structure, deoxy-oximidine retains potent anti-cancer activity and may therefore offer a promising starting point for semi-synthetic diversification of the macrolactone ring. Overall, our findings highlight the exceptional catalytic versatility of PKS domains in *trans*-AT PKSs and open up new avenues for the production of novel benzolactone enamide anti-cancer agents via biosynthetic engineering.

Acknowledgements

This work was supported by the Research Foundation – Flanders (FWO) through a research grant (G061821N) and an infrastructure grant (I002720N). For the NMR calculations performed in this work, resources and services were provided by the VSC (Flemish Supercomputer Center), funded by the FWO and the Flemish Government.

Keywords: biosynthesis • bacterial natural products • genome mining • polyketides • enzymology

- [1] D. J. Newman, G. M. Cragg, *J. Nat. Prod.* **2020**, *83*, 770–803.
- [2] C. T. Walsh, *Science* **2004**, *303*, 1805–1810.
- [3] M. A. Fischbach, C. T. Walsh, *Chem. Rev.* **2006**, *106*, 3468–3496.
- [4] C. Hertweck, *Angew. Chem. Int. Ed.* **2009**, *48*, 4688–4716.
- [5] L. Du, L. Lou, *Nat. Prod. Rep.* **2010**, *27*, 255–278.
- [6] J. N. E. Helfrich, J. Piel, *Nat. Prod. Rep.* **2016**, *33*, 231–316.
- [7] J. W. Kim, K. Shin-Ya, K. Furihata, Y. Hayakawa, H. Seto, *J. Org. Chem.* **1999**, *64*, 153–155.
- [8] Y. Hayakawa, T. Tomikawa, K. Shin-Ya, N. Arai, K. Nagai, K. I. Suzuki, K. Furihata, *J. Antibiot. (Tokyo)* **2003**, *56*, 905–908.
- [9] Y. Hayakawa, T. Tomikawa, K. Shin-Ya, N. Arai, K. Nagai, K. I. Suzuki, *J. Antibiot. (Tokyo)* **2003**, *56*, 899–904.
- [10] M. R. Boyd, C. Farina, P. Belfiore, S. Gagliardi, J. W. Kim, Y. Hayakawa, J. A. Beutler, T. C. McKee, B. J. Bowman, E. J. Bowman, *J. Pharmacol. Exp. Ther.* **2001**, *297*, 114–120.
- [11] M. P. Collins, M. Forgac, *Biochim. Biophys. Acta Biomembr.* **2020**, *1862*, 183341.
- [12] M. Pérez-Sayáns, J. M. Somoza-Martín, F. Barros-Angueira, J. M. G. Rey, A. García-García, *Cancer Treat. Rev.* **2009**, *35*, 707–713.
- [13] M. Huss, H. Wieczorek, *J. Exp. Biol.* **2009**, *212*, 341–346.
- [14] S. P. Niehs, B. Dose, S. Richter, S. J. Pidot, H. M. Dahse, T. P. Stinear, C. Hertweck, *Angew. Chem. Int. Ed.* **2020**, *59*, 7766–7771.
- [15] R. Ueoka, R. A. Meoded, A. Gran-Scheuch, A. Bhushan, M. W. Fraaije, J. Piel, *Angew. Chem. Int. Ed.* **2020**, *59*, 7761–7765.
- [16] Y. Zhu, Q. Zhang, S. Li, Q. Lin, P. Fu, G. Zhang, H. Zhang, R. Shi, W. Zhu, C. Zhang, *J. Am. Chem. Soc.* **2013**, *135*, 18750–18753.

- [17] N. Liu, L. Song, M. Liu, F. Shang, Z. Anderson, D. J. Fox, G. L. Challis, Y. Huang, *Chem. Sci.* **2016**, *7*, 482–488.
- [18] W. L. Kelly, C. A. Townsend, *J. Am. Chem. Soc.* **2002**, *124*, 8186–8187.
- [19] A. Beaton, C. Lood, E. Cunningham-Oakes, A. MacFadyen, A. J. Mullins, W. El Bestawy, J. Botelho, S. Chevalier, S. Coleman, C. Dalzell, S. K. Dolan, A. Faccenda, M. G. K. Ghequire, S. Higgins, A. Kutschera, J. Murray, M. Redway, T. Salih, A. C. da Silva, B. A. Smith, N. Smits, R. Thomson, S. Woodcock, M. Welch, P. Cornelis, R. Lavigne, V. van Noort, N. P. Tucker, *FEMS Microbiol. Lett.* **2018**, *365*, fny069.
- [20] X. Wang, E. J. Bowman, B. J. Bowman, J. A. Porco, *Angew. Chem. Int. Ed.* **2004**, *43*, 3601–3605.
- [21] N. Grimblat, M. M. Zanardi, A. M. Sarotti, *J. Org. Chem.* **2015**, *80*, 12526–12534.
- [22] M. Jenner, J. P. Afonso, C. Kohlhaas, P. Karbaum, S. Frank, J. Piel, N. J. Oldham, *Chem. Comm.* **2016**, *52*, 5262–5265.
- [23] K. Blin, S. Shaw, A. M. Kloosterman, Z. Charlop-Powers, G. P. Van Wezel, M. H. Medema, T. Weber, *Nucleic Acids Res.* **2021**, *49*, W29–W35.
- [24] D. T. Wagner, J. Zeng, C. B. Bailey, D. C. Gay, F. Yuan, H. R. Manion, A. T. Keatinge-Clay, *Structure* **2017**, *25*, 1045–1055.e2.
- [25] Y. Zou, H. Yin, D. Kong, Z. Deng, S. Lin, *ChemBioChem* **2013**, *14*, 679–683.
- [26] F. P. Guengerich, *ACS Catal.* **2018**, *8*, 10964–10976.
- [27] C. M. Schneider, K. Khownum, W. Li, J. T. Spletstoser, T. Haack, G. I. Georg, *Angew. Chem. Int. Ed.* **2011**, *50*, 7855–7857.
- [28] R. Shen, C. T. Lin, E. J. Bowman, B. J. Bowman, J. A. Porco, *J. Am. Chem. Soc.* **2003**, *125*, 7889–7901.
- [29] I. I. Turnaev, K. V. Gunbin, V. V. Suslov, I. R. Akberdin, N. A. Kolchanov, D. A. Afonnikov, *Plants* **2020**, *9*, 1092.
- [30] M. W. Fraaije, N. M. Kamerbeek, W. J. H. Van Berkel, D. B. Janssen, *FEBS Lett.* **2002**, *518*, 43–47.
- [31] H. L. Schubert, R. M. Blumenthal, X. Cheng, *Trends Biochem. Sci.* **2003**, *28*, 329–335.
- [32] D. C. Gay, P. J. Spear, A. T. Keatinge-Clay, *ACS Chem. Biol.* **2014**, *9*, 2374.
- [33] L. E. N. Quadri, P. H. Weinreb, M. Lei, M. M. Nakano, P. Zuber, C. T. Walsh, *Biochemistry* **1998**, *37*, 1585–1595.
- [34] P. C. Dorrestein, S. B. Bumpus, C. T. Calderone, S. Garneau-Tsodikova, Z. D. Aron, P. D. Straight, R. Kolter, C. T. Walsh, N. L. Kelleher, *Biochemistry* **2006**, *45*, 12756.
- [35] M. Kline, D. Pierce, S. Cheatham, *Magn. Reson. Chem.* **2017**, *55*, 154–156.
- [36] A. A. Mokhir, K. V. Domasevich, N. Kent Dalley, X. Kou, N. N. Gerasimchuk, O. A. Gerasimchuk, *Inorganica Chim. Acta* **1999**, *284*, 85–98.
- [37] G. Cecere, C. M. König, J. L. Alleva, D. W. C. MacMillan, *J. Am. Chem. Soc.* **2013**, *135*, 11521–11524.
- [38] J. Masschelein, P. K. Sydor, C. Hobson, R. Howe, C. Jones, D. M. Roberts, Z. Ling Yap, J. Parkhill, E. Mahenthiralingam, G. L. Challis, *Nat. Chem.* **2019**, *11*, 906–912.

